





BRIEF REPORT | JANUARY 25 2024

Madrid-2019 force field: An extension to divalent cations Sr^{2+} and Ba^{2+} ✓

S. Blazquez ; Ian C. Bourg ; C. Vega  



J. Chem. Phys. 160, 046101 (2024)

<https://doi.org/10.1063/5.0186233>

 CHORUS



View
Online



Export
Citation

Articles You May Be Interested In

On the compatibility of the Madrid-2019 force field for electrolytes with the TIP4P/Ice water model

J. Chem. Phys. (December 2024)

The Madrid-2019 force field for electrolytes in water using TIP4P/2005 and scaled charges: Extension to the ions F^- , Br^- , I^- , Rb^+ , and Cs^+

J. Chem. Phys. (January 2022)

Maximum in density of electrolyte solutions: Learning about ion–water interactions and testing the Madrid-2019 force field

J. Chem. Phys. (April 2022)

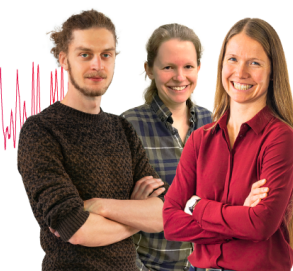
Webinar From Noise to Knowledge

May 13th – Register now



Zurich
Instruments

Universität
Konstanz



Madrid-2019 force field: An extension to divalent cations Sr^{2+} and Ba^{2+}

Cite as: J. Chem. Phys. 160, 046101 (2024); doi: 10.1063/5.0186233

Submitted: 5 November 2023 • Accepted: 27 December 2023 •

Published Online: 25 January 2024



S. Blazquez,¹ Ian C. Bourg,^{2,3} and C. Vega^{1,a)}

AFFILIATIONS

¹ Dpto. Química Física I, Fac. Ciencias Químicas, Universidad Complutense de Madrid, 28040 Madrid, Spain

² Department of Civil and Environmental Engineering, Princeton University, Princeton, New Jersey 08544, USA

³ High Meadows Environmental Institute, Princeton University, Princeton, New Jersey 08544, USA

^{a)} Author to whom correspondence should be addressed: cvega@quim.ucm.es

ABSTRACT

In this work, we present a parameterization of Sr^{2+} and Ba^{2+} cations, which expands the alkali earth set of cations of the Madrid-2019 force field. We have tested the model against the experimental densities of eight different salts, namely, SrCl_2 , SrBr_2 , SrI_2 , $\text{Sr}(\text{NO}_3)_2$, BaCl_2 , BaBr_2 , BaI_2 , and $\text{Ba}(\text{NO}_3)_2$. The force field is able to reproduce the experimental densities of all these salts up to their solubility limit. Furthermore, we have computed the viscosities for two selected salts, finding that the experimental values are overestimated, but the predictions are still reasonable. Finally, the structural properties for all the salts have been calculated with this model and align remarkably well with experimental observations.

Published under an exclusive license by AIP Publishing. <https://doi.org/10.1063/5.0186233>

When simulating aqueous electrolyte solutions using classical Molecular Dynamics (MD) or Monte Carlo (MC) simulations, both a force field for water and a force field for ions are needed. In the case of liquid water, we have shown in previous works that the TIP4P/2005 model is able to predict a wide range of properties, such as the density, viscosity, temperature of maximum density (TMD), and interfacial tension.¹ In the case of ions, the story is somewhat different and there is a great variety of force fields to choose from.^{2–19}

Among these force fields, some use scaled charges for ions (i.e., an effective charge lower than ± 1 per unit of formal charge). The use of scaled charges was proposed by Leontyev and Stuchebukhov²⁰ who suggested a value of ± 0.75 (in electron units) for the charge of the ions. Later, Kann and Skinner²¹ also recommended the use of scaled charges, but they proposed different charges depending on the employed water force field. The use of scaled charges has been supported by different authors in recent years,^{17–19,22–27} leading to models with scaled charges between ± 0.75 and ± 1 for describing the potential energy surface but with formal charges when describing the dipole moment surface.^{28,29}

Indeed, we also started to develop force fields for ions optimized for use with the TIP4P/2005 water model and based on the idea of using a scaled charge of ± 0.85 for monovalent ions. In this

context, we started the Madrid-2019 force field, which now comprises a wide variety of ions, including, among the cations, all the alkali metals, ammonium and the alkaline earth Ca^{2+} and Mg^{2+} and, in the case of the anions, all the halogens as well as the sulfate and nitrate ions.^{17,24,30} All salts resulting from the combination of these ions can be modeled by using the Madrid-2019 force field, which has been shown to be able to reproduce a wide variety of properties of aqueous solutions much more accurately than unit charge models.^{31–37} For these reasons, in this work, we have developed a force field for Sr^{2+} and Ba^{2+} using scaled charges to expand the set of alkali earth metals. The parameters developed here should help advance examinations of Sr^{2+} and Ba^{2+} in a variety of applications, including as tracers of elemental cycling in Geosciences^{38–40} and as target elements in synchrotron x-ray characterizations of metal coordination in a wide variety of materials.^{41–44}

We have adjusted the cation–water interactions to reproduce the experimental densities of eight water-soluble salts [i.e., SrCl_2 , SrBr_2 , SrI_2 , $\text{Sr}(\text{NO}_3)_2$, BaCl_2 , BaBr_2 , BaI_2 , and $\text{Ba}(\text{NO}_3)_2$]; then, we have adjusted the cation–anion interactions to keep a low number of contact ion pairs (CIPs) and to avoid precipitation at the experimental solubility limit of each salt. In Table I, we present the force field parameters for barium and strontium; the parameters for the rest of the ions can be found in Refs. 17, 24, and 30 and in the

TABLE I. Force field parameters for strontium and barium salts. O_n and O_w refer to the oxygen atom of nitrate and water, respectively, and N_n refers to the nitrogen atom of the nitrate group. Numbers in boldface indicate that the interactions follow the LB rules. The parameters for the rest of the ions are found in Refs. 17, 24, and 30.

Atom	Sr^{2+}		Ba^{2+}	
	$q = +1.7$		$q = +1.7$	
	σ_{ij} (Å)	ϵ_{ij} (kJ/mol)	σ_{ij} (Å)	ϵ_{ij} (kJ/mol)
Sr^{2+}	3.0500	0.4550	3.1578	0.4293
Ba^{2+}	3.1578	0.4293	3.2656	0.4050
Cl^-	3.3000	0.8000	3.8000	0.5000
Br^-	3.5800	0.6000	3.9000	0.4000
I^-	3.6000	0.4000	4.2000	0.3000
O_n	2.9550	0.6321	3.3000	0.5900
N_n	3.1000	0.5688	3.2078	0.5366
O_w	2.6800	4.5000	2.9680	3.4000

supplementary material or in the topology file provided within this article. It is important to mention that following the philosophy of the Madrid-2019 original force field, the ion–water and the ion–ion interactions in general do not follow Lorentz–Berthelot (LB) combining rules. Thus, these interactions are explicitly defined. Notice that the sulfate and fluoride barium and strontium salts have not been studied in this work because their solubilities are less than 10^{-2} mol/kg at room temperature and pressure.

To calculate densities and structural properties, we employed a system comprised of 555 water molecules and the corresponding number of ions for the desired molality, m (defined as moles of solute per kilogram of water). The hydration number (HN) and the number of contact ion pairs (CIPs) were computed from the corresponding radial distribution function (RDF). For instance, CIPs were calculated as follows:

$$CIP = 4\pi\rho_{\pm} \int_0^{r_{\min}} g_{\pm}(r)r^2 dr, \quad (1)$$

where $g_{\pm}(r)$ is the cation–anion RDF, r_{\min} is the position of the first minimum of the integrated RDF, and ρ_{\pm} is the lower number density after dissociation (in this work, the number density of the cation). The results quantify the number of cations in contact with a single anion (the number of anions in contact with a single cation can be obtained by multiplying reported CIP numbers by 2). Note also that it is important to simultaneously plot the cation–anion and cation– O_w RDFs to determine if one is really evaluating the CIP or a solvent separated ion pair (SSIP). For the case of the hydration number, the evaluation is similar, but we used the cation–water RDF and the number density of water. In the case of viscosity calculations, we employed a larger system of 4440 water molecules and the corresponding number of ions. To compute the viscosity, we followed the methodology developed by Gonzalez and Abascal.⁴⁵ First, we performed a NpT simulation of 20 ns to calculate accurately the volume of the system. After that, we carried out a NVT simulation of 50 ns using the average volume obtained in the NpT simulation.

The pressure tensor $p_{\alpha\beta}$ was calculated every 2 fs. Finally, we used the Green–Kubo formula for the shear viscosity η ,

$$\eta = \frac{V}{kT} \int_0^{\infty} \langle p_{\alpha\beta}(0) p_{\alpha\beta}(t) \rangle_{t_0} dt, \quad (2)$$

where V is the volume of the system, k is the Boltzmann constant, T is the temperature, and $p_{\alpha\beta}$ is the non-diagonal components of the pressure tensor. The upper limit of the integral was usually between 10 and 20 ps.

For all simulations, we used the GROMACS package.⁴⁶ The leap-frog integrator algorithm⁴⁷ was employed with a time step of 2 fs. We also applied periodic boundary conditions in all directions for all runs. To keep constant the temperature and pressure, we employed the Nosé–Hoover thermostat^{48,49} and an isotropic Parrinello–Rahman barostat,⁵⁰ both with a coupling constant of 2 ps. For electrostatic and van der Waals interactions, we used a cutoff radius of 1.0 nm with long-range corrections in the energy and pressure applied to the Lennard–Jones (LJ) part of the potential. The particle mesh ewald method (PME)⁵¹ was used to account for the long-range electrostatic forces. We used the LINCS algorithm^{52,53} to maintain water geometry.

As previously mentioned, our force field, following the methodology of previous works,^{17,24,54} was developed to reproduce the densities of all the salts considered in this work up to their solubility limit (see the supplementary material where experimental solubilities for each salt have been collected). In Fig. 1, we show the densities as a function of concentration for the different strontium and barium salts studied. For the strontium salts [Fig. 1(a)], predicted densities accurately reproduce the experiments with a slight overestimation for $SrCl_2$ and SrI_2 at high concentrations. Note that for SrI_2 , there were no available data close to the experimental solubility limit and we show an extrapolation of the experimental data (dashed line). To assess the impact of system size and cutoff on our calculations, we performed a simulation of a 2 m $SrCl_2$ solution. This simulation involved a system eight times larger, consisting of 4440 water molecules, and employed a cutoff of 1.6 nm. Remarkably, we observed nearly identical results compared to those obtained with a smaller system and a 1.0 nm cutoff [see Fig. 1(a) and the supplementary material]. This reaffirms that there are no discernible finite size or cutoff effects influencing the density calculations of this work. For the case of barium salts [Fig. 1(b)], experimental densities are also well reproduced, with a slight overestimation at high concentrations for $BaBr_2$ and BaI_2 .

Once we have verified that the force field reproduces experimental densities, we examine the viscosities of the salts. In previous works, we have shown that scaled charge models improve the description of viscosities compared to unit charge models. However, even a charge of ± 0.85 leads to an overestimation of the experimental viscosity and we found that for monovalent ions it was necessary to use a charge of ± 0.75 .^{54,57} If this is true, one can ask why we have chosen a charge of ± 0.85 (i.e., ± 1.7 for the divalent cations Sr^{2+} and Ba^{2+}) for our force field. The answer is that this charge, on average, yields a better overall description of several properties of aqueous solutions. Based on our previous work, it is expected that our new force field for Sr^{2+} and Ba^{2+} should overestimate the experimental viscosities but in a reasonable way. In Fig. 2, we present viscosity results for both $SrCl_2$ and $BaCl_2$. As anticipated, an overestimation

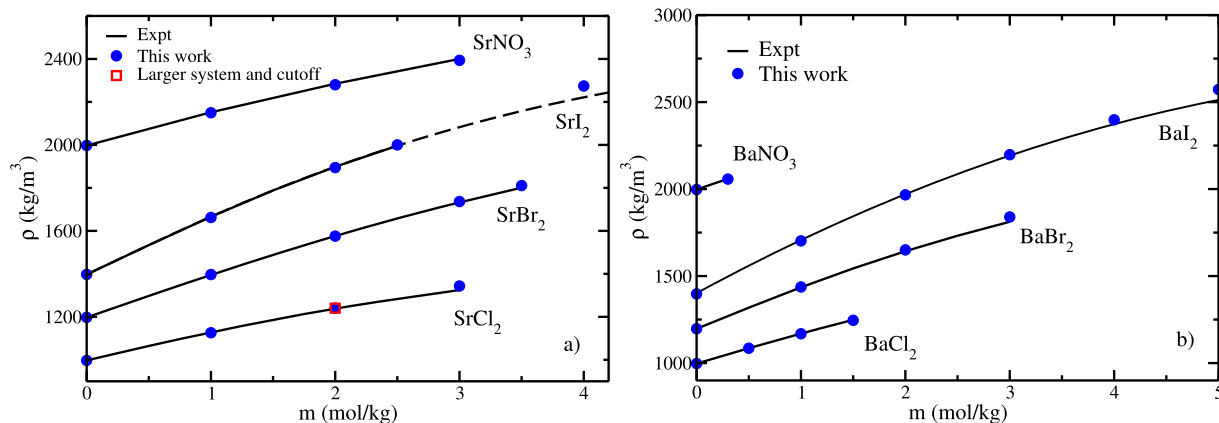


FIG. 1. Densities of (a) strontium and (b) barium salts at $T = 298.15$ K and 1 bar by using the Madrid-2019 force field. Blue circles: Madrid-2019 force field. Red square: system of 4440 water molecules and simulated with a cutoff of 1.6 nm. Black solid lines: fit of experimental data taken from Refs. 55 and 56. Bromide, iodide, and nitrate salts values were shifted up 200, 400, and 1000 density units, respectively, for better legibility. The concentration of salt is given in molality units, m (i.e., number of mol of salt per kg of water).

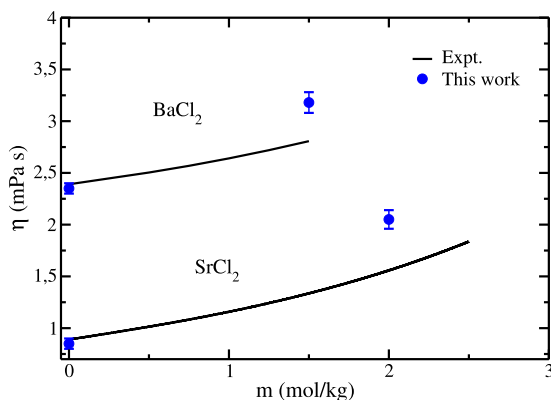


FIG. 2. Viscosities of SrCl_2 and BaCl_2 salts at $T = 298.15$ K and 1 bar by using the Madrid-2019 force field. Blue circles: Madrid-2019 force field. Black solid lines: fit of experimental data taken from Ref. 55. BaCl_2 values were shifted up 1.5 viscosity units for better legibility.

of the experimental results is observed. This aligns with the conclusion of our recent work,⁵⁷ which showed that no single charge scaling factor is able to simultaneously reproduce all structural and dynamic properties of salt solutions, and in this case, a lower scaled charge would enable an improved match to experimental viscosity results.

Finally, we have studied the structural features of the model (see Table II) focusing on the number of CIP, the cation–water distance, and the hydration number of the cation. First, it is evident that our model exhibits a low number of CIP, effectively preventing salt precipitation. If we now examine the cation–water distances calculated from the first peak of the corresponding RDF, the predicted $d_{\text{Sr-Ow}}$ value of 2.60 Å falls within the range reported by experiments.^{58–63} Barium, owing to its larger size, naturally exhibits

TABLE II. Structural properties for strontium and barium electrolyte solutions at 298.15 K and 1 bar: number of contact ion pairs (CIPs) per anion, hydration number of the cation (HNc), and position of the first maximum of the cation–water RDF ($d_{\text{c-Ow}}$). Experimental data from Refs. 58–63 are given in parentheses.

Salt	m (mol/kg)	CIP	HNc	$d_{\text{c-Ow}}$ (Å)
SrCl_2	3.0	0.14	7.7 (7.3–10.3)	2.60 (2.50–2.64)
SrBr_2	3.5	0.01	8.0 (7.3–10.3)	2.60 (2.50–2.64)
SrI_2	2.5	0.04	8.0 (7.3–10.3)	2.60 (2.50–2.64)
$\text{Sr}(\text{NO}_3)_2$	1	0.04	7.8 (7.3–10.3)	2.60 (2.50–2.64)
BaCl_2	1.5	0.02	9.0 (7.8–9.3)	2.85 (2.75–2.90)
BaBr_2	3	0.13	8.6 (7.8–9.3)	2.84 (2.75–2.90)
BaI_2	5	0.12	8.5 (7.8–9.3)	2.85 (2.75–2.90)
$\text{Ba}(\text{NO}_3)_2$	0.3	0.06	8.9 (7.8–9.3)	2.84 (2.75–2.90)

a larger distance, with $d_{\text{Ba-Ow}}$ of 2.84 Å. Importantly, even in the case of barium, the model-calculated distances remain consistent with experimental observations. Likewise, the cation hydration calculations yield insightful results. Strontium ions are typically surrounded by an average of eight water molecules, whereas barium ions, due to their greater size, exhibit a slightly larger hydration shell, encompassing ~ 8.7 water molecules. Remarkably, these hydration numbers closely align with experimental data, mirroring the consistency observed in cation–water distances. Note that when the CIP increases, HNc decreases reflecting the fact that some water molecules of the first hydration layer are replaced by anions. In summary, our force field successfully reproduces the structural characteristics of these cations, achieving congruence with experimental findings. Indeed, in the supplementary material, we present the cation–water RDFs and draw comparisons with the findings of Pappalardo *et al.*⁵⁸ We note favorable agreement not only in the positioning of the first peak but also in that of subsequent peaks. While

our study exhibits slightly higher intensity in peak heights compared to their work, the overall results remain remarkably similar.

As a conclusion, in this work, we present an extension of the Madrid-2019 force field expanding the set of alkali earth metals with the Sr^{2+} and Ba^{2+} cations. The model presented in this study is able to reproduce the experimental densities of strontium and barium halide salts up to their solubility limit. The force field also accurately reproduces the experimental structural features of the studied salts and provides reasonable results for viscosities. We hope that this extension of the Madrid-2019 force field will be a valuable resource for the scientific community engaged in modeling electrolyte solutions. The force field now includes F^- , Cl^- , Br^- , I^- , SO_4^{2-} , NO_3^- , Li^+ , Na^+ , K^+ , Rb^+ , Cs^+ , Ca^{2+} , Mg^{2+} , Sr^{2+} , Ba^{2+} , and NH_4^+ .

In the supplementary material, we have collected the numerical densities and viscosities of the studied salts and the RDFs mentioned in the main text and we also provide a topology file of the complete Madrid-2019 force field.

This project was funded by the Ministry of Science, Innovation and Universities under Grant No. PID2022-136919NB-C31. I.C.B. was supported by the U.S. Department of Energy, Office of Science, Office of Basic Energy Sciences, Geosciences program under Award No. DE-SC0018419.

AUTHOR DECLARATIONS

Conflict of Interest

The authors have no conflicts to disclose.

Author Contributions

S. Blazquez: Conceptualization (equal); Data curation (lead); Formal analysis (equal); Investigation (equal); Methodology (equal); Writing – original draft (equal); Writing – review & editing (equal).
Ian C. Bourg: Conceptualization (equal); Methodology (equal); Resources (equal); Writing – review & editing (equal).
C. Vega: Conceptualization (lead); Funding acquisition (equal); Investigation (equal); Methodology (equal); Supervision (equal); Writing – original draft (equal); Writing – review & editing (equal).

DATA AVAILABILITY

The data that support the findings of this study are available within the article and its supplementary material.

REFERENCES

- C. Vega and J. L. F. Abascal, *Phys. Chem. Chem. Phys.* **13**, 19663 (2011).
- W. R. Smith, I. Nezbeda, J. Kolafa, and F. Moučka, *Fluid Phase Equilib.* **466**, 19 (2018).
- J. Chandrasekhar, D. C. Spellmeyer, and W. L. Jorgensen, *J. Am. Chem. Soc.* **106**, 903 (1984).
- D. E. Smith and L. X. Dang, *J. Chem. Phys.* **100**, 3757 (1994).
- K. P. Jensen and W. L. Jorgensen, *J. Chem. Theory Comput.* **2**, 1499 (2006).
- P. J. Lenart, A. Jusufi, and A. Z. Panagiotopoulos, *J. Chem. Phys.* **126**, 044509 (2007).
- I. S. Joung and T. E. Cheatham, *J. Phys. Chem. B* **112**, 9020 (2008).
- D. Corradini, M. Rovere, and P. Gallo, *J. Chem. Phys.* **132**, 134508 (2010).
- H. Yu, T. W. Whitfield, E. Harder, G. Lamoureux, I. Vorobyov, V. M. Anisimov, A. D. MacKerell, Jr., and B. Roux, *J. Chem. Theory Comput.* **6**, 774 (2010).
- M. B. Gee, N. R. Cox, Y. Jiao, N. Benteinitis, S. Weerasinghe, and P. E. Smith, *J. Chem. Theory Comput.* **7**, 1369 (2011).
- S. Mamatkulov, M. Fyta, and R. R. Netz, *J. Chem. Phys.* **138**, 024505 (2013).
- F. Moučka, I. Nezbeda, and W. R. Smith, *J. Chem. Theory Comput.* **9**, 5076 (2013).
- P. T. Kiss and A. Baranyai, *J. Chem. Phys.* **141**, 114501 (2014).
- J. Kolafa, *J. Chem. Phys.* **145**, 204509 (2016).
- I. Pethes, *J. Mol. Liq.* **242**, 845 (2017).
- T. Yagasaki, M. Matsumoto, and H. Tanaka, *J. Chem. Theory Comput.* **16**, 2460 (2020).
- S. Blazquez, M. M. Conde, J. L. F. Abascal, and C. Vega, *J. Chem. Phys.* **156**, 044505 (2022).
- R. Fuentes-Azcatl and J. Alejandro, *J. Phys. Chem. B* **118**, 1263 (2014).
- P. Habibi, J. R. T. Postma, J. T. Padding, P. Dey, T. J. H. Vlugt, and O. A. Moulτος, *Ind. Eng. Chem. Res.* **62**, 11992 (2023).
- I. V. Leontyev and A. A. Stuchebrukhov, *J. Chem. Phys.* **130**, 085102 (2009).
- Z. R. Kann and J. L. Skinner, *J. Chem. Phys.* **141**, 104507 (2014).
- M. Kohagen, P. E. Mason, and P. Jungwirth, *J. Phys. Chem. B* **118**, 7902 (2014).
- T. Martinek, E. Duboué-Dijon, Š. Timr, P. E. Mason, K. Baxová, H. E. Fischer, B. Schmidt, E. Pluhařová, and P. Jungwirth, *J. Chem. Phys.* **148**, 222813 (2018).
- I. M. Zeron, J. L. F. Abascal, and C. Vega, *J. Chem. Phys.* **151**, 134504 (2019).
- M. Soniat, G. Pool, L. Franklin, and S. W. Rick, *Fluid Phase Equilib.* **407**, 31 (2016).
- Y. Yao, M. L. Berkowitz, and Y. Kanai, *J. Chem. Phys.* **143**, 241101 (2015).
- F. Wang, O. Akin-Ojo, E. Pinnick, and Y. Song, *Mol. Simul.* **37**, 591 (2011).
- C. Vega, *Mol. Phys.* **113**, 1145 (2015).
- S. Blazquez, J. L. Abascal, J. Lagerweij, P. Habibi, P. Dey, T. J. Vlugt, O. A. Moulτος, and C. Vega, *J. Chem. Theory Comput.* **19**, 5380 (2023).
- V. M. Trejos, M. de Lucas, C. Vega, S. Blazquez, and F. Gámez, *J. Chem. Phys.* **159**, 224501 (2023).
- S. Blazquez, I. M. Zeron, M. M. Conde, J. L. F. Abascal, and C. Vega, *Fluid Phase Equilib.* **513**, 112548 (2020).
- L. F. Sedano, S. Blazquez, E. G. Noya, C. Vega, and J. Troncoso, *J. Chem. Phys.* **156**, 154502 (2022).
- G. L. Breton and L. Joly, *J. Chem. Phys.* **152**, 241102 (2020).
- L. Perin and P. Gallo, *J. Phys. Chem. B* **127**, 4613 (2023).
- F. Gámez, L. F. Sedano, S. Blazquez, J. Troncoso, and C. Vega, *J. Mol. Liq.* **377**(1), 121433 (2023).
- S. Blazquez, C. Vega, and M. Conde, *J. Mol. Liq.* **383**(1), 122031 (2023).
- L. Yan, D. Scott, and G. Balasubramanian, *J. Mol. Liq.* **390**, 123198 (2023).
- W. Wei and T. J. Algeo, *Geochim. Cosmochim. Acta* **287**, 341 (2020).
- J. G. Wiederhold, *Environ. Sci. Technol.* **49**, 2606 (2015).
- L. C. Nielsen, J. J. De Yoreo, and D. J. DePaolo, *Geochim. Cosmochim. Acta* **115**, 100 (2013).
- J. N. Bracco, S. S. Lee, J. E. Stubbs, P. J. Eng, S. Jindra, D. M. Warren, A. Kommu, P. Fenter, J. D. Kubicki, and A. G. Stack, *J. Phys. Chem. C* **123**, 1194 (2018).
- S. S. Lee, C. Park, N. C. Sturchio, and P. Fenter, *J. Phys. Chem. Lett.* **11**, 4029 (2020).
- P. D'Angelo, V. Migliorati, F. Sessa, G. Mancini, and I. Persson, *J. Phys. Chem. B* **120**, 4114 (2016).
- N. Sahai, S. A. Carroll, S. Roberts, and P. A. O'Day, *J. Colloid Interface Sci.* **222**, 198 (2000).
- M. A. González and J. L. F. Abascal, *J. Chem. Phys.* **132**, 096101 (2010).
- D. van der Spoel, E. Lindahl, B. Hess, G. Groenhof, A. E. Mark, and H. J. C. Berendsen, *J. Comput. Chem.* **26**, 1701 (2005).
- D. Beeman, *J. Comput. Phys.* **20**, 130 (1976).
- S. Nosé, *Mol. Phys.* **52**, 255 (1984).
- W. G. Hoover, *Phys. Rev. A* **31**, 1695 (1985).
- M. Parrinello and A. Rahman, *J. Appl. Phys.* **52**, 7182 (1981).

- ⁵¹U. Essmann, L. Perera, M. L. Berkowitz, T. Darden, H. Lee, and L. G. Pedersen, *J. Chem. Phys.* **103**, 8577 (1995).
- ⁵²B. Hess, H. Bekker, H. J. C. Berendsen, and J. G. E. M. Fraaije, *J. Comput. Chem.* **18**, 1463 (1997).
- ⁵³B. Hess, *J. Chem. Theory Comput.* **4**, 116 (2008).
- ⁵⁴P. Habibi, A. Rahbari, S. Blazquez, C. Vega, P. Dey, T. J. H. Vlugt, and O. A. Moulτος, *J. Phys. Chem. B* **126**, 9376 (2022).
- ⁵⁵M. Liliberte and W. E. Cooper, *J. Chem. Eng. Data* **49**, 1141 (2004).
- ⁵⁶E. W. Washburn, C. J. West, and National Research Council (U.S.), *International Critical Tables of Numerical Data, Physics, Chemistry and Technology* (McGraw-Hill, New York, 1928).
- ⁵⁷S. Blazquez, M. M. Conde, and C. Vega, *J. Chem. Phys.* **158**, 054505 (2023).
- ⁵⁸R. R. Pappalardo, D. Z. Caralampio, J. M. Martínez, and E. Sanchez Marcos, *Inorg. Chem.* **60**, 13578 (2021).
- ⁵⁹P. D'Angelo, N. Pavel, D. Roccatano, and H.-F. Nolting, *Phys. Rev. B* **54**, 12129 (1996).
- ⁶⁰V. Migliorati, A. Caruso, and P. D'Angelo, *Inorg. Chem.* **58**, 14551 (2019).
- ⁶¹R. Caminiti, A. Musinu, G. Paschina, and G. Pinna, *J. Appl. Crystallogr.* **15**, 482 (1982).
- ⁶²S. Ramos, G. W. Neilson, A. C. Barnes, and M. J. Capitán, *J. Chem. Phys.* **118**, 5542 (2003).
- ⁶³T. M. Seward, C. M. B. Henderson, J. M. Charnock, and T. Driesner, *Geochim. Cosmochim. Acta* **63**, 2409 (1999).